Martensitic transformation of a Ni-Al alloy. II. Theoretical treatments

Y. Yamada
Institute for Solid State Physics, The University of Tokyo, Roppongi, Tokyo 106, Japan

Y. Noda* and K. Fuchizaki†
Faculty of Engineering Science, Osaka University, Toyonaka, Osaka 560, Japan

(Received 26 April 1990)

The seven-layered martensite structure of the Ni-Al alloy reported in the preceding paper is investigated on a theoretical basis. We have developed a treatment of the martensite phase transformation within a site-independent scheme describing atomic fluctuations in a highly anharmonic lattice. From a microscopic viewpoint a pseudospin variable is introduced which stands for the amplitude of the local vibrational mode called the embryonic mode, and the martensite transformation is discussed as the ordering process of the pseudospins. Through a coarse-graining procedure, a semimacroscopic view has also been developed within the Ginzburg-Landau formalism. The results have been applied to analyze the observed neutron-diffraction spectra. In particular, the anomalous incommensurability of the spectra is understood by considering that the order parameter takes on two different values alternatively in space, which is interpreted in terms of the theoretically predicted "crest-riding-periodon" phase.

I. INTRODUCTION

It has been well established that the thermoelastic martensite phase transformations of bcc-based alloys are associated with the inherent lattice instability of these alloys[1] manifested by the low-lying (soft) TA phonon branches along the [110] and the [211] directions.[2–5] From this viewpoint, the martensite structure is expressible in terms of the displacement field of "soft"-phonon modes, which is supplemented by some uniform bulk strains.

The most commonly observed martensite structures are the so-called $2H$ and $9R$ structures, which are understood by the freezing of the TA phonon modes with the wave vector $\mathbf{q}=\frac{1}{2}[110]$, and $\mathbf{q}=\frac{1}{3}[110]$, respectively. Generally speaking, one may be able to expect the existence of other soft modes. In 1986, Shapiro *et al.*[6] carried out neutron inelastic scattering measurements on Ni_xAl_{1-x} alloys with a Ni concentration of $x\sim 0.6$. They observed a remarkable softening of the TA phonon branch around $\mathbf{q}=\frac{1}{7}[110]$, which suggests that, in this particular case of Ni-Al alloys, the martensite structure could be expressible in terms of the freezing of the TA mode with $\mathbf{q}=\frac{1}{7}[110]$.

In fact, a structure analysis of this material was already carried out by Martynov *et al.*[7] They proposed the structure characterized by the $(5,\bar{2})$ stacking (using Zhudanov's notation[8]) of the (110) atomic planes along the [110] direction. This is consistent with the view described above in that the periodicity of the proposed structure is seven layers along the [110] direction as is expected by the freezing of the mode with $\mathbf{q}=\frac{1}{7}[110]$. However, the atomic positions of the proposed structure are not simply represented by the normal coordinate of the TA soft mode.

Recently, Noda *et al.*[9] carried out an extensive neutron-diffraction measurement on the Ni-Al alloy.[10] (Paper I of this series of papers, referred to as I hereafter.) They provided a more complete set of intensity data and revealed various new aspects in the characteristics of the observed neutron spectra. The results are summarized as follows.

(i) Lattice parameters. The lattice symmetry is reconfirmed to be monoclinic with the lattice parameters

$$\begin{aligned} a_m &= 4.172\ \text{Å}\ , \\ b_m &= 2.690\ \text{Å}\ , \\ c_m &= 14.450\ \text{Å}\ , \\ \bar{\beta}_m &= 94.10^\circ\ . \end{aligned} \tag{1.1}$$

(ii) Anomalous incommensurability. The peak positions of Bragg reflections are not completely indexed by the above monoclinic lattice. That is, the peak positions of each Bragg reflection are slightly shifted from the commensurate reciprocal-lattice points along the $[001]_m$ direction. The shift from the commensurate positions is commonly observed in various kinds of incommensurate structures. However, the amount of the shift in the present case does not show any simple regularity, as it should when the structure is expressed by some kind of incommensurate long-period structure.

(iii) Line broadening and splitting. The spectra of the Bragg reflections show appreciable line broadening. The amount of the broadening depends on the index of the reflection. Not only that, some of the peaks exhibit splittings into double-peak structure. The overall feature of the splitting seems to suggest that there are two kinds of monoclinic lattices with different monoclinic angles given by

$$\beta_m^{(1)}=94.37^\circ\ ,$$
$$\beta_m^{(2)}=93.82^\circ\ . \tag{1.2}$$

[The $\bar{\beta}_m$ given in (1.1) is the "average" of these two values.]

These experimental results are certainly out of the scope of the conventional interpretation of the martensite structure in terms of the frozen soft-phonon mode. Recently, Yamada and co-workers proposed an alternative view to describe the martensitic transformation.[11,12] They took the local vibrational modes, rather than phonons, as the basis functions to expand the energy of a highly anharmonic lattice. The local coordinate is shown to be represented by a three-state pseudospin variable, whence they called the model a "pseudospin description" of martensitic transformation.

They applied this model to investigate two kinds of martensite structures. Besides the most popular case of $9R$, they specifically investigated the case of the Ni-Al alloys. The preliminary results proved that the calculated ordered phase of the pseudospins correctly gives the atomic arrangements of the structure proposed by Martynov *et al.*[7] This has been recently reconfirmed by Noda *et al.*[9,10] using the more extensive intensity data of neutron diffraction. It would, therefore, be reasonable to take this alternative view to discuss the new experimental aspects which have not been understood by the conventional soft-phonon concept.

The purpose of the present paper is to extend the theoretical treatment of the pseudospin model and to discuss the newly obtained experimental features described above. The paper is constructed as follows: In Sec. II, the theoretical backgrounds based on the pseudospin description of the highly anharmonic lattice have been established from both microscopic and semimacroscopic (thermodynamical) standpoints. In particular, the latter is necessary to provide the basis of the discussions on anomalous incommensurability, etc. In Sec. III, we reinvestigate the "averaged" martensite structure by identifying the martensite phase to be the "ferro"-type ordered phase of pseudospins. In Sec. IV, we discuss the details of the observed neutron spectra, such as anomalous incommensurability, broadening, and splitting of the diffraction spectra, based on the thermodynamical standpoint developed in Sec. II. Section V is devoted to the summary and discussions.

II. THEORETICAL BACKGROUND

A. Microscopic view: Pseudospin variable

The martensitic phase transformation of bcc-based alloys is associated with the inherent lattice instability of these alloys which manifests itself as the low-lying TA phonon branch along the [110] direction.

The problem of martensitic phase transformation may be, in a broad sense, considered to be the problem concerning the lattice dynamical properties of a highly anharmonic lattice. Generally speaking, there are two alternative standpoints from which to discuss the lattice dynamics of an anharmonic lattice.[13]

(i) Mode-independent scheme. The energy of the system is expanded by taking the harmonic phonon modes as basis functions as follows:

$$H=\tfrac{1}{2}\sum_{\mathbf{q},s}[P^2(\mathbf{q},s)+\omega^2(\mathbf{q},s)Q^2(\mathbf{q},s)] + \sum_{\substack{\mathbf{q}_1,\mathbf{q}_2,\mathbf{q}_3\\ s_1,s_2,s_3}} A(\mathbf{q}_1,s_1,\mathbf{q}_2,s_2,\mathbf{q}_3,s_3) \times Q(\mathbf{q}_1,s_1)Q(\mathbf{q}_2,s_2)Q(\mathbf{q}_3,s_3) \times\delta(\mathbf{q}_1+\mathbf{q}_2+\mathbf{q}_3)+\cdots\ . \tag{2.1}$$

In this scheme, the anharmonicity is included in the higher-order coupling terms between phonon modes. The summation runs over the wave vector $\mathbf{q}$ and the branch index s.

(ii) Site-independent scheme. The energy is (approximately) expressed as follows:

$$H=\tfrac{1}{2}\sum_{i,\mu}P_i^{\mu 2}+\sum_{i,\mu}V_{\rm loc}^s(Q_i^\mu)+\sum_{\substack{i,j\\ \mu;\nu}}C_{ij}^{\mu\nu}Q_i^\mu Q_j^\nu\ . \tag{2.2}$$

Here, Q_i^μ is the μth local vibrational mode of a cluster of atoms located around the ith site. $V_{\rm loc}^s(Q_i^\mu)$ is the single cluster potential for the local mode Q_i^μ. $V_{\rm loc}^s$ is considered to be highly anharmonic. $C_{ij}^{\mu\nu}$ gives the intersite interaction between Q_i^μ and Q_j^ν, which is assumed to be harmonic. The summation runs over the site index i instead of q.

The phonon-mode description is more conventionally used. However, let us adopt the latter scheme as the basis of the following discussions.

As was discussed in previous papers,[11,12] we make the following basic assumption: From the observed soft-phonon mode, one can extract a specific local mode Q_i^μ which is particularly relevant to the martensitic phase transformation. This mode is identified to be the mode which *locally* simulates the *ABC*-type (or fcc-type) stacking of hexagonal basal planes. As was discussed in Ref. 11, in the specific case of Ni-Al [the $\frac{1}{7}(110)$ soft phonon mode], we can identify the local mode to be the "tilting" mode of a cluster of atoms composed of six (110) layers. (See Fig. 1.)

Let us call this specific local mode the "embryonic mode," $Q_i^{\rm emb}$. The implication is that the local distortion plays the role of the "embryo" of the low-temperature martensite structure. Once $Q_i^{\rm emb}$ is defined as above, we can extract, from the total Hamiltonian given in Eq. (2.2), the terms which are particularly relevant to the phase transition from the following considerations.

(i) $V_{\rm loc}^s(Q_i^\mu)$. Among the local single-cluster potentials, we consider the term $V_{\rm loc}^s(Q_i^{\rm emb})$. The local potential will be characterized by a three-minimum structure as given in Fig. 2. The side minima just correspond to the energy of the "tilted" configuration which locally simulates *ABC*-type stacking of hexagonal basal planes. In fact, a recent theoretical calculation of $V(Q_i^{\rm emb})$ by Wentzkovitch and Cohen[14] clearly shows the three-minimum structure.

At this stage, let us simplify the system by assuming

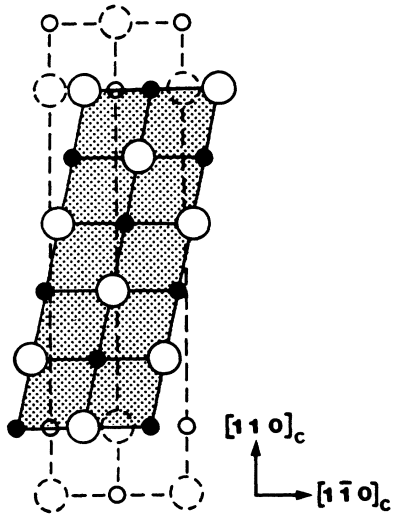

FIG. 1. The embryonic mode postulated from the soft phonon in NiAl. The mode is characterized by the "tilting" motion of a cluster composed of six $(110)_c$ layers.

that $Q_i^{\rm emb}$ can only take on three discrete values: $Q=0$ and $\pm Q_0$. (See Fig. 2.) It is convenient to introduce a three-state pseudospin variable σ_i which takes the values $\sigma=(0,+1,-1)$. The value of $Q_i^{\rm emb}$ can be represented by the pseudospin σ_i, where $\sigma_i=0,1,-1$ corresponds to $Q_i^{\rm emb}=0,+Q_0,-Q_0$, respectively. $V_{\rm loc}^s(Q_i^{\rm emb})$ is then simply given by

$$V_{\rm loc}^s(Q_i^{\rm emb})=\varepsilon\sigma_i^2 , \tag{2.3}$$

where ε is the difference between the energy of the stable state ($Q=0$) and the metastable states ($Q=\pm Q_0$). Since $Q=\pm Q_0$ correspond to the local "embryo" states, the energy ε may be called the embryo creation energy.

Other $V_{\rm loc}^s(Q_i^{\mu})$'s which are not directly relevant to the phase transition may be taken to be harmonic:

$$V_{\rm loc}^s(Q_i^{\mu})\simeq\kappa_{\mu}Q_i^{\mu 2} . \tag{2.4}$$

(ii) $C_{ij}^{\mu\nu}Q_i^{\mu}Q_j^{\nu}$. As for the intersite interaction terms, we note that $Q_i^{\rm emb}$ will couple strongly to the transverse translational mode of the neighboring cluster as a whole, $Q_{i+1}^{\rm tr}$. This situation is depicted in Fig. 3. When both of the two neighboring clusters take on the same "tilted" state, $\sigma=1$, the atoms at the interface layers come too close to each other, which is relaxed by the relative transverse motion of the clusters into the opposite directions. (See Fig. 3.)

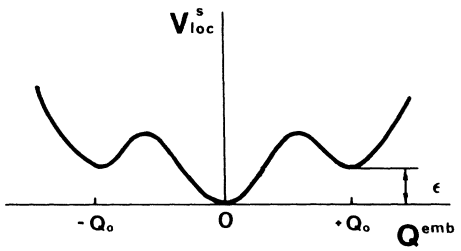

FIG. 2. Assumed single-cluster potential for the embryonic mode. At $Q^{\rm emb}=\pm Q_0$, there are side minima (metastable states) corresponding to the stable *ABC*-type stacking configuration of the basal planes.

Therefore, we only retain the intersite interaction term between $Q_i^{\rm emb}$ and $Q_{i+1}^{\rm tr}$:

$$\sum_{\substack{i,j\\ \mu,\nu}} C_{ij}^{\mu\nu}Q_i^{\mu}Q_j^{\nu}=\alpha\sum_i \sigma_i(Q_i^{\rm tr}-Q_{i+1}^{\rm tr}) , \tag{2.5}$$

where we have taken into account only the nearest-neighbor interaction and have used the following simplified notation:

$$\alpha\equiv C_{i\,i+1}^{\rm emb\,tr} . \tag{2.6}$$

Based on these considerations, the Hamiltonian (2.2) has been greatly simplified to give

$$H=\varepsilon\sum_i \sigma_i^2+\kappa\sum_i Q_i^{\rm tr2}+\alpha\sum_i \sigma_i(Q_i^{\rm tr}-Q_{i+1}^{\rm tr}) . \tag{2.7}$$

As was discussed in a previous paper,[11] the above expres-

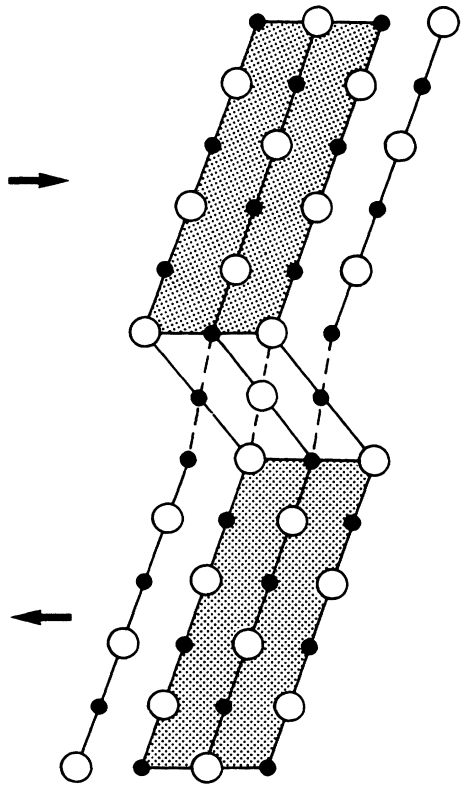

FIG. 3. Origin of the coupling between $Q^{\rm emb}$ and $Q^{\rm tr}$. The translation of the neighboring clusters in the opposite directions as shown by the arrows is favorable for the same tilted configuration ($\sigma=1$) of the clusters (and vice versa) because the atomic positions at the interface layers come too close to each other without this translation.

sion is further simplified to give the following effective pseudospin Hamiltonian:

$$H=\tilde{\varepsilon}\sum_i \sigma_i^2-\tilde{J}\sum_i \sigma_i\sigma_{i+1} , \tag{2.8}$$

where $\tilde{\varepsilon}$ and $\tilde{J}$ are the effective embryo creation energy and the effective embryo-embryo interaction energy, respectively, and are given by

$$\tilde{\varepsilon}=\varepsilon-\frac{\alpha^2}{2\kappa} ,$$
$$\tilde{J}=\frac{\alpha^2}{2\kappa} . \tag{2.9}$$

Once the effective pseudospin Hamiltonian is established as above, one can follow the conventional statistical-mechanical treatment to discuss the phase-transition scheme of Ni-Al. The mean-field approximation (MFA) treatment describes the cooperative ordering process of the spins. The ordered phase is given by the "ferro"-type spin order with the averaged spin value $\langle\sigma\rangle$ given by

$$\langle\sigma\rangle=\frac{2\sinh(\tilde{J}\langle\sigma\rangle/k_BT)}{e^{\tilde{\varepsilon}/k_BT}+2\cosh(\tilde{J}\langle\sigma\rangle/k_BT)} , \tag{2.10}$$

as well as the transverse translation $\langle Q^{\rm tr}\rangle$,

$$\langle|Q^{\rm tr}|\rangle=\frac{\alpha}{\kappa}\langle\sigma\rangle , \tag{2.11}$$

which is proportional to $\langle\sigma\rangle$. Physically, $\langle Q^{\rm tr}\rangle$ gives the bulk shear strain perpendicular to the $[110]_c$ direction. In Sec. III, the above results will be utilized to construct the structure of the martensite phase by identifying the martensite phase to be the ferro-type ordered phase of the pseudospin system.

B. Semimacroscopic aspects: Crest-riding periodon

As will be seen later, it is necessary to establish a thermodynamical view within the Ginzburg-Landau (GL) scheme in order to discuss the details of the observed results beyond the averaged structure. In this subsection, we deduce the GL-type free-energy functional, which provides the basis of the discussions on the experimental results such as shifts and broadenings of the Bragg peaks. In the GL scheme, the order parameter ξ is allowed to be spatially varied. In the present system, such a spatially varying order parameter is defined by going through the "coarse-graining" procedure of the pseudospin σ_i as follows.[15] Within the MFA, the local free energy associated with the local ordering $\langle\sigma_i\rangle$ is expressed by[16]

$$f(\langle\sigma_i\rangle)=-\tfrac{1}{2}\sum_{i,j}\tilde{J}\langle\sigma_i\rangle\langle\sigma_j\rangle+\frac{1}{\beta}\sum_i\int_0^{\langle\sigma_i\rangle}\tanh^{-1}g(\sigma)d\sigma , \tag{2.12}$$

where $g(\sigma)$ is given by

$$g(\sigma)=\frac{\sigma e^{\beta\tilde{\varepsilon}}+\sigma[\sigma^2e^{\beta\tilde{\varepsilon}}+4(1-\sigma^2)]^{1/2}}{\sigma^2e^{\beta\tilde{\varepsilon}}+[\sigma^2e^{\beta\tilde{\varepsilon}}+4(1-\sigma^2)]^{1/2}} . \tag{2.13}$$

We expand $\tanh^{-1}(\sigma)$ in a power series of σ:

$$\tanh^{-1}g(\sigma)=\tilde{g}_1\sigma+\tilde{g}_3\sigma^3+\tilde{g}_5\sigma^5 , \tag{2.14}$$

where $\tilde{g}$'s are explicitly given in terms of the microscopic parameter $\tilde{\varepsilon}$ as follows:

$$\tilde{g}_1=\tfrac{1}{2}(e^{\beta\tilde{\varepsilon}}+2) ,$$
$$\tilde{g}_3=-\tfrac{1}{48}(e^{\beta\tilde{\varepsilon}}-4)(e^{\beta\tilde{\varepsilon}}+2)^2 , \tag{2.15}$$
$$\tilde{g}_5=\tfrac{1}{1280}(3e^{5\beta\tilde{\varepsilon}}-40e^{3\beta\tilde{\varepsilon}}+240e^{\beta\tilde{\varepsilon}}+256) .$$

When these expansion coefficients are actually evaluated, one sees that the leading term in $\tilde{g}_3$ is negative while $\tilde{g}_5$ is positive definite for $T>0$. We must, therefore, keep the terms up to the fifth order in σ in the expansion so as to avoid the unphysical instability.

In order to go through coarse-graining procedure, we introduce the Fourier transform of $\langle\sigma_i\rangle$, $\langle\sigma(q)\rangle$, through

$$\langle\sigma(q)\rangle=\frac{1}{N}\sum_j\langle\sigma_j\rangle e^{iqj} . \tag{2.16}$$

The first term of Eq. (2.12) is then expressed by

$$-\tfrac{1}{2}\sum_{i,j}\tilde{J}\langle\sigma_i\rangle\langle\sigma_j\rangle=-\frac{N}{2}\sum_q\tilde{J}(q)\langle|\sigma(q)|^2\rangle , \tag{2.17}$$

where $\tilde{J}(q)$ is the Fourier transform of the interaction and is given explicitly by

$$\tilde{J}(q)=\sum_j^{nn}\tilde{J}e^{iqJ}=2\tilde{J}\cos q \simeq 2\tilde{J}(1-\tfrac{1}{2}q^2) . \tag{2.18}$$

The last procedure is justified because higher q components should be averaged out in the context of the coarse graining of $\langle\sigma_i\rangle$. Through such a coarse-graining procedure, a spatially continuous order parameter $\xi(x)$ is defined by

$$\xi(x)=\frac{L}{2\pi}\int\langle\sigma(q)\rangle e^{iqx}dq . \tag{2.19}$$

By using (2.18) and (2.19), the total free energy is expressed in the standard GL formalism

$$F[\xi(x)]=\int\left[\frac{\lambda}{2}(\partial_x\xi)^2+\hat{f}(\xi)\right]dx ,$$
$$\hat{f}(\xi)=\frac{a}{2}\xi^2+\frac{b}{4}\xi^4+\frac{c}{6}\xi^6 , \tag{2.20}$$

where the coefficients are given by

$$\lambda=\tilde{J} ,$$
$$a=k_BT\tilde{g}_1-2\tilde{J} ,$$
$$b=k_BT\tilde{g}_3 , \tag{2.21}$$
$$c=k_BT\tilde{g}_5 ,$$

where $\lambda>0$, $b<0$, and $c>0$. The free energy (2.20) describes a first-order phase-transition process as the temperature is varied. The transition temperature obtained

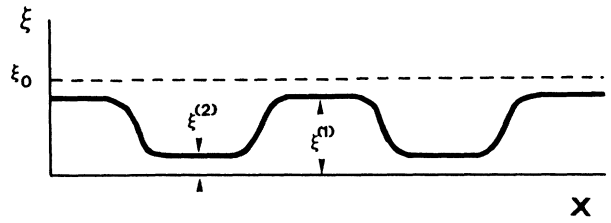

FIG. 4. The spatial variation of $\xi(x)$ in the CRP state. The order parameter takes on two discrete values $\xi^{(1)}$ and $\xi^{(2)}$ alternatively. The size of a single "domain" is considered to be of semimacroscopic scale.

from (2.21) is, as it should be, consistent with that given by the direct evaluation on a microscopic basis using Eq. (2.10).[15] When the temperature dependences of the parameters b and c are neglected, Eq. (2.20) reduces to the conventional phenomenological expression which has been used in various problems including spinodal decomposition process, etc.[17]

The spatially varying order parameter $\xi(x)$ is obtained by solving the Euler equation

$$\lambda\frac{\partial^2\xi}{\partial x^2}-\frac{d\hat{f}}{d\xi}=0 \tag{2.22}$$

under appropriate boundary conditions.

Recently, several authors[18–21] discussed the properties of the spatial variation of the order parameter using the phenomenologically postulated GL equation which has the form as Eq. (2.20). Falk[18] pointed out that in the one-dimensional (1D) system, there is a possible solution in which the order parameter $\xi(x)$ takes on two different values, $\xi^{(1)}$ and $\xi^{(2)}$, alternatively as the coordinate x is varied. That is, the order parameter spatially oscillates between $\xi^{(1)}$ and $\xi^{(2)}$. (See Fig. 4.) This solution has been obtained under the following boundary conditions:

$$\left.\begin{array}{c}\partial_x\xi=0,\\ \xi=\bar{\xi},\ \hat{f}(\bar{\xi})=\mu\end{array}\right\}\ \text{as } x\to\pm\infty\ , \tag{2.23}$$

where μ is a finite positive value. (See Fig. 5.)

Barsch and Krumhansl[20,21] extended the discussions to the 2D system and obtained essentially the same solution, and specifically called it a crest-riding-periodon (CRP) solution. As is shown schematically in Fig. 6 of Ref. 21,

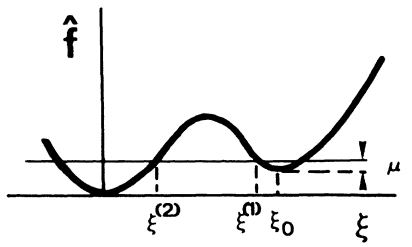

FIG. 5. The free-energy density just above the phase-transition temperature. In the CRP state, the system has a constant local energy given by the thin horizontal line $[f=f(\xi_0)+\mu]$, which makes $\xi(x)$ oscillate between $\xi^{(1)}$ and $\xi^{(2)}$.

the solution, in fact, is "riding" on the "crest" of the local free-energy surface. This solution is definitely not the most stable state, but it may exist as a metastable phase when the boundary conditions (2.23) are appropriate. In Sec. IV, this particular solution will be discussed in connection with the shift and broadening of the diffraction spectra.

III. AVERAGED STRUCTURE: FERRO-TYPE ORDERED PHASE OF PSEUDOSPINS

In this section, we investigate the averaged structure of the martensite phase, neglecting the details of the observed diffraction spectra much as anomalous incommensurability, broadening, and splitting. Based on the discussions in the preceding section, the martensite phase should be characterized by the ferro-type ordered structure of the pseudospins. That is, all of the clusters are in the same "tilted" configuration. At the same time, the lattice is spontaneously strained because of the strong coupling of the pseudospins to the strain components. The positions of the atom in the martensite phase are therefore given by

$$\mathbf{r}_{ik}=(1+\epsilon)\cdot\mathbf{r}_i^0+\mathbf{r}_k^0+\mathbf{u}_k,\quad k=0,1,\ldots,6\ , \tag{3.1}$$

where $\mathbf{r}_i^0$ is the position vector of the origin of the ith unit cell, $\mathbf{r}_k^0$ is that of the atom in the kth layer in the original bcc lattice, ϵ is the strain tensor, and $\mathbf{u}_k$ is the internal displacement of the kth layer due to the embryo creation. Referring to the discussions in the previous section, $\mathbf{u}_k$ is given in terms of the order parameter $\xi\ (=\langle\sigma\rangle)$ by

$$\mathbf{u}_k=\xi\mathbf{e}_k^{\text{emb}}\ , \tag{3.2}$$

where $\mathbf{e}_k^{\text{emb}}$ is the eigenvector of the embryonic mode. As is easily seen in Fig. 1, $\mathbf{e}_k^{\text{emb}}$ is expressed by

$$\mathbf{e}_k^{\text{emb}}=\begin{cases}\sqrt{2/35}(k-\frac{2}{7})\mathbf{e}_1, & k=1,2,\ldots,6,\\ 0 \quad k=0\ ,\end{cases} \tag{3.3}$$

where $\mathbf{e}_1$ is the unit vector along the $[1\bar{1}0]_c$ direction. The layer specified by $k=0$ is the interface layer which does not belong to the embryo cluster.

Using Eqs. (3.2) and (3.3), we have the explicit expression of the internal displacement $\mathbf{u}_k$ given by

$$\mathbf{u}_k=(k-\tfrac{2}{7})u_{\text{int}}\mathbf{e}_1(1-\delta_{0k}),\quad k=0,1,\ldots,6\ , \tag{3.4}$$

$$u_{\text{int}}=\xi\hat{u}_{\text{int}}\ , \tag{3.5}$$

where u_{int} is the relative internal displacement of the neighboring layers in the ordered phase with an arbitrary order-parameter value ξ, and $\hat{u}_{\text{int}}$ corresponds to the value in the perfectly ordered state of $\xi=1$, which forms the "ideal" $(5,\bar{2})$ stacking discussed later.

Thus, the position vector $\mathbf{r}_{ik}$ in the martensite phase is given by

$$\mathbf{r}_{ik}=(1+\epsilon)\cdot\mathbf{r}_i^0+\mathbf{r}_k^0+(k-\tfrac{2}{7})u_{\text{int}}\mathbf{e}_1(1-\delta_{0k})\ ,\quad k=0,1,\ldots,6\ . \tag{3.6}$$

Here, ϵ and u_{int} are the parameters to be determined by

the comparison with the experimental results.

In order to obtain the strain tensor components, it is convenient to define a monoclinic lattice frame within the undistorted bcc structure as follows:

$$\begin{aligned} \mathbf{a}_m^0 &= \mathbf{a}_c - \mathbf{b}_c \ , \\ \mathbf{b}_m^0 &= -\mathbf{c}_c \ , \\ \mathbf{c}_m^0 &= 3\mathbf{a}_c + 4\mathbf{b}_c \ . \end{aligned} \tag{3.7}$$

The monoclinic unit cell defined as above is depicted in Fig. 6(a). The actual values for the lattice constants are given by

$$\begin{aligned} a_m^0 &= \sqrt{2}a_0 = 4.042 \text{ Å} \ , \\ b_m^0 &= a_0 = 2.858 \text{ Å} \ , \\ c_m^0 &= 5a_0 = 14.290 \text{ Å} \ , \\ \beta_m^0 &= -\tan^{-1}7 = 98.13^\circ \ . \end{aligned} \tag{3.8}$$

In I, it was shown that, in the martensite phase, these values have been changed to

$$\begin{aligned} a_m &= 4.172 \text{ Å} \ , \\ b_m &= 2.690 \text{ Å} \ , \\ c_m &= 14.450 \text{ Å} \ , \\ \bar{\beta}_m &= 94.10^\circ \ . \end{aligned} \tag{3.9}$$

Using these values, the bulk deformation associated with the cubic-monoclinic transition is expressed by the following strain tensor[22] referring to the orthogonal lattice frame defined by $\mathbf{e}_1 \| [1\bar{1}0]_c$, $\mathbf{e}_2 \| [001]_c$, $\mathbf{e}_3 \| [110]_c$:

$$\epsilon = \begin{bmatrix} 0.0322 & 0 & 0.0744 \\ 0 & -0.0588 & 0 \\ 0 & 0 & 0.0188 \end{bmatrix} . \tag{3.10}$$

The only remaining parameter u_{int} should be determined by comparing the observed intensity $I(\mathbf{K})$ with the calculated structure factor

$$F(\mathbf{K}) = \sum_{\mathbf{K}_h} \sum_{k,k'=0}^{6} b_{k^{(\prime)}} e^{i\mathbf{K}\cdot\mathbf{r}_{k^{(\prime)}}(u_{\text{int}})} \delta(\mathbf{K}-\mathbf{K}_h) \ , \tag{3.11}$$

where $\mathbf{K}_h$ is a reciprocal-lattice point of the monoclinic lattice (a_m, b_m, c_m) and $\mathbf{r}_k(u_{\text{int}})$ is given by

$$\begin{aligned} \mathbf{r}_{k^{(\prime)}}(u_{\text{int}}) &= \mathbf{r}^0_{k^{(\prime)}} + (k - \tfrac{7}{2})u_{\text{int}}\mathbf{e}_1(1-\delta_{0k}) \ , \\ \mathbf{r}^0_k &= \frac{k}{14}\mathbf{a}_m + \frac{k}{7}\mathbf{c}_m \ , \\ \mathbf{r}^0_{k'} &= r^0_k + \tfrac{1}{2}\mathbf{a}_m + \tfrac{1}{2}\mathbf{b}_m \ . \end{aligned} \tag{3.12}$$

This procedure has already been carried out in I, and excellent agreement with the experimental results has been obtained by taking

$$u_{\text{int}} = 0.0794 \ . \tag{3.13}$$

As is depicted in Fig. 6, the obtained structure is characterized by the so-called $(5,\bar{2})$ stacking sequence. Notice, however, that this notation has not been used in the strict sense of Zhdanov's formalism; the ideal $(5,\bar{2})$ stacking sequence should represent the sequence of $|ABCABCB|ABCABCB|$ stacking of the hexagonal layers. [See Fig. 6(c).]

In order to obtain the ideal $(5,\bar{2})$ structure, it is easily shown that the following parameter values should be

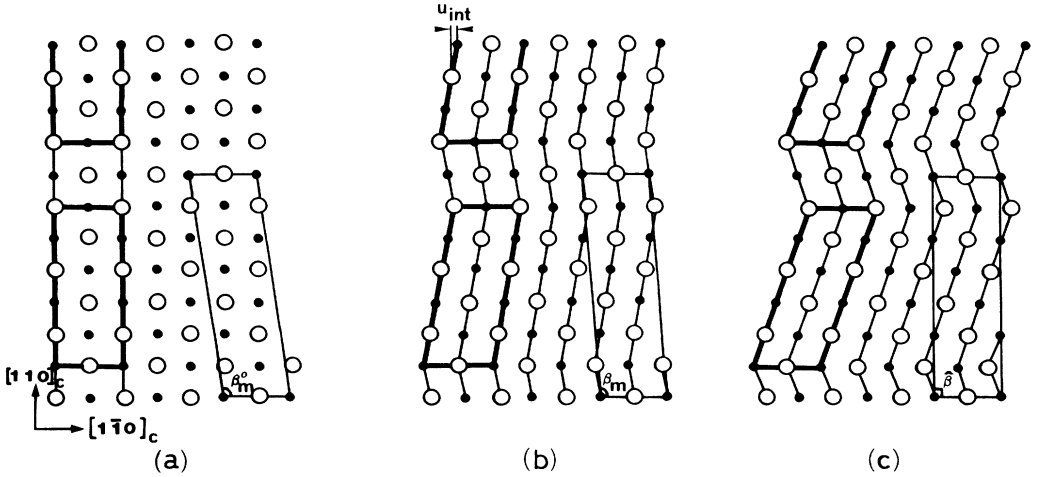

FIG. 6. Construction of the $(5,\bar{2})$ structure. (a) The original bcc lattice where all clusters are in the $\sigma=0$ state. The monoclinic unit cell (a_m^0, b_m^0, c_m^0) defined in the text is indicated on the right-hand corner ($\beta_m^0 = 98.13^\circ$). (b) The observed $(5,\bar{2})$ structure. All clusters are in the tilted configuration. At the same time, the lattice is uniformly distorted ($\beta_m = 94.10^\circ$). (c) The ideal $(5,\bar{2})$ structure given by *ABCABCB* stacking of the hexagonal layers. The original monoclinic lattice is deformed to construct an orthorhombic lattice ($\hat{\beta} = 90^\circ$).

TABLE I. Parameter values to specify the atomic positions in the ferro-type ordered phase given in Eq. (3.7) in text. The observed parameter values are approximately $\frac{1}{2}$ of the ideal $(5,\bar{2})$ stacking structure. The value of $u_{\rm int}$ is given in the unit of a_m.

	Ideal	Obs.	Obs./ideal
$u_{\rm int}$	0.1667	0.0794	0.48
ϵ_{11}	0.0607	0.0322	0.53
ϵ_{22}	−0.134	−0.0588	0.44
ϵ_{33}	0	+0.0188	
ϵ_{13}	0.1428	0.0744	0.52

realized:

$$\epsilon_{11}=\frac{3}{2\sqrt{2}}-1=0.0607\ ,$$
$$\epsilon_{22}=\frac{\sqrt{3}}{2}-1=-0.134\ ,$$
$$\epsilon_{33}=0\ , \tag{3.14}$$
$$\epsilon_{13}=\tfrac{1}{7}=0.1428\ ,$$
$$\hat{u}_{\rm int}=\tfrac{1}{6}=0.166\ .$$

The observed parameter values are tabulated in Table I in comparison with those of the ideal $(5,\bar{2})$ structure. It is noticed that all of the observed parameter values (except for ϵ_{33}) are approximately $\frac{1}{2}$ of the "ideal" values. In particular, we notice that the shear strain ϵ_{13} just corresponds to $\langle Q^{\rm tr}\rangle$ discussed in the previous section. Therefore, the above results suggest that $\langle Q^{\rm tr}\rangle$ couples linearly to the order parameter ξ ($=\langle\sigma\rangle$) which is consistent with Eq. (2.11).

At this stage, the reason why the obtained order-parameter value remains to be about one-half of the ideal value is not known. This point will be discussed later in Sec. V.

IV. SHIFTS AND BROADENINGS OF THE DIFFRACTION SPECTRA: CRP STRUCTURE

So far, we have considered the averaged structure assuming that the system is spatially homogeneous. On the other hand, as was pointed out in I, there are appreciable broadenings (sometimes even splittings) of the peak profiles as well as irregular shifts of the peak position from the regular commensurate positions. The observed patterns of the peak shift and the broadening are given in I, one of which is reproduced in Fig. 7. These features definitely suggest that the system does not have a spatially uniform and regular structure but exhibits some sort of spatial irregularity or modulation. In the following, we discuss the properties of spatial variation of the structure which are consistent with the observed results.

The most remarkable characteristic of the pattern of the peak shift (and broadening) seen in Fig. 7 is that it shows regular repetition along the $[001]_m$ direction with the period of $7c_m^*$. That is,

$$I(\mathbf{K})\simeq I(\mathbf{K}+7\mathbf{c}_m^*)\ . \tag{4.1}$$

As is given in the Appendix, this characteristic is simply due to the fact that the atomic layers are regularly spaced along the $[110]_c$ direction even in the inhomogeneous structure.

Therefore, the spatial inhomogeneity of the structure is associated with the parameter along the $[1\bar{1}0]_c$ direction, or the x value in the monoclinic frame. Since the position vector r_{ik} is generally expressed by Eq. (3.6), we have

$$x_{ik}=x_{ik}^0+(\epsilon\cdot\mathbf{r}_i^0)_x+(k-\tfrac{7}{2})u_{\rm int}(1-\delta_{0k})\ ,$$
$$k=0,1,\ldots,6\ . \tag{4.2}$$

Here, the parameter $u_{\rm int}$ describes the internal displacement which is proportional to the order parameter of the pseudospin system [see Eq. (3.2)]:

$$u_{\rm int}\propto\langle\sigma\rangle=\xi\ , \tag{4.3}$$

while ϵ is the bulk strain induced by the ordering of the pseudospins.

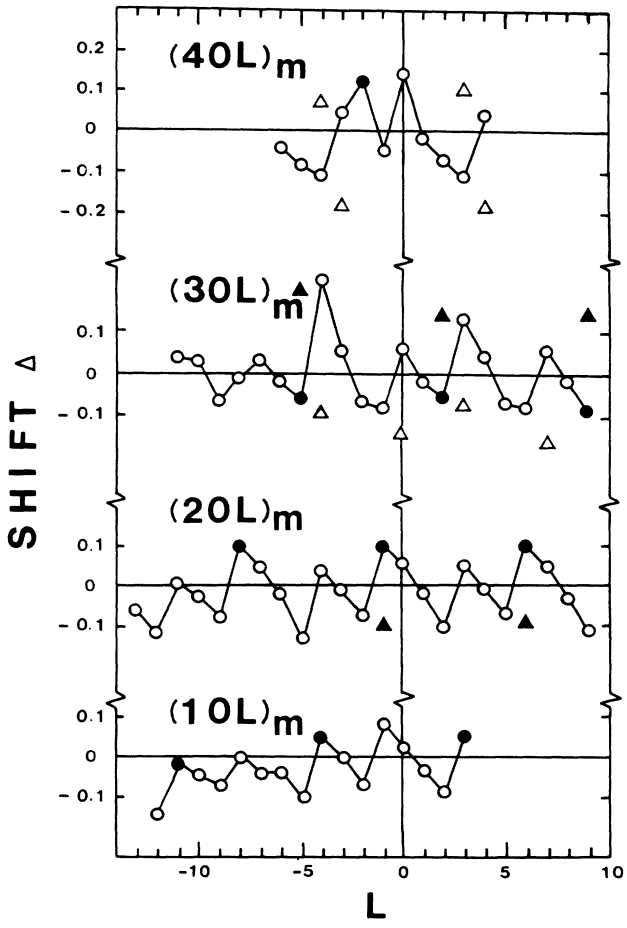

FIG. 7. The observed shift pattern of the peak position from the commensurate reciprocal-lattice points of the average monoclinic lattice. The solid circles give the original bcc Bragg reflections. The triangles indicate the positions of the minor peaks when the spectra show the double-peak feature.

In the previous section, defining the averaged structure, the parameter $u_{\rm int}$ and ϵ are taken to be constant throughout the system. In order to describe the inhomogeneity of the structure, we now consider that these parameters are r dependent. Thus, x_{ik} is given by

$$x_{ik}=x_{ik}^0+[\epsilon(\mathbf{r}_i^0)\cdot\mathbf{r}_i^0]_x+(k-\tfrac{7}{2})u_{\rm int}(\mathbf{r}_i^0)(1-\delta_{0k}) . \tag{4.4}$$

From Eq. (4.3), the r dependent $u_{\rm int}$ implies that, in the inhomogeneous structure, the order parameter ξ is spatially modulated.

Furthermore, we have to notice that, in the present system, the order parameter is coupled linearly to the shear strain ϵ_{13}. [See (2.11).] Hence, the inhomogeneity of the structure is considered to be essentially due to the spatial modulation of the order parameter $\xi(r)$. The characteristic length scale of the spatial variation of ξ is of the order of the inverse width of the broadening of the Bragg reflections. Referring to Fig. 6 of I, the length scale of the spatial variation should reach as long as 300 Å ($\sim 20\times c_m$) which means that the modulation period is of semimacroscopic size. As was discussed in Sec. II, the possibility of the stabilization of the state with a spatially modulated order parameter called the crest-riding-periodon phase has been pointed out by several authors. Since the GL equation we derived in Sec. II has exactly the same form as the one which these authors phenomenologically postulated, one expects that the present system may stabilize the crest-riding-periodon phase.

In this connection, it is important to notice the following experimental results: As was discussed in I, the general feature of the diffraction spectra can be understood by considering the coexistence of two monoclinic lattices with different monoclinic angles given by

$$\begin{aligned}\beta_m^{(1)}&=94.37^\circ ,\\ \beta_m^{(2)}&=93.82^\circ .\end{aligned} \tag{4.5}$$

Since the monoclinic angle β_m is directly related to ϵ_{13} by

$$\epsilon_{13}=(\cos\beta_m-\cos\beta_m^0) , \tag{4.6}$$

the above fact indicates that there are semimacroscopic regions of differently strained lattices with

$$\begin{aligned}\epsilon_{13}^{(1)}&=0.0696 ,\\ \epsilon_{13}^{(2)}&=0.0794 .\end{aligned} \tag{4.7}$$

Therefore, it would not be unreasonable to consider that the observed inhomogeneous state is identified to be the predicted CRP phase[23] where the order parameter ξ, whence the internal displacement parameter $u_{\rm int}$, is spatially oscillating between two different values $\xi^{(1)}$ and $\xi^{(2)}$ as well as the shear strain. Using the proportionality between ξ and ϵ_{13} and the values included in Table I, the corresponding parameter values of $u_{\rm int}$ are estimated to be

$$\begin{aligned}u_{\rm int}^{(1)}&=0.0743 ,\\ u_{\rm int}^{(2)}&=0.0847 .\end{aligned} \tag{4.8}$$

Summarizing these results, we construct a possible model of the inhomogeneous structure as follows: The system is given by the coherent mixture of the two kinds of domains with slightly different monoclinic structures defined, respectively, by

$$x_{ik}^{(\nu)}=x_{ik}^0+\epsilon_{11}x_i^0+\epsilon_{13}^{(\nu)}z_i^0+(k-\tfrac{7}{2})u_{\rm int}^{(\nu)}(1-\delta_{0k}) ,\qquad k=0,1,\ldots,6,\quad \nu=1,2 \tag{4.9}$$

with

$$\begin{aligned}u_{\rm int}^{(1)}&=0.0743 ,\\ \epsilon_{13}^{(1)}&=0.0696 ,\end{aligned} \tag{4.10}$$

$$\begin{aligned}u_{\rm int}^{(2)}&=0.0847 ,\\ \epsilon_{13}^{(2)}&=0.0794 .\end{aligned} \tag{4.10'}$$

Notice that, due to the difference in $u_{\rm int}^{(\nu)}$, these two structures are internally different rather than just specified by the monoclinic angle $\beta_m^{(\nu)}$.

The observed pattern of the shift and broadening should be compared with the following diffraction spectra of the CRP state:

$$\begin{aligned}I(\mathbf{K})&=\sum_{\nu=1}^{2}\sum_{K_h^{(\nu)}}|F(\mathbf{K})|^2\delta(K-K_h^{(\nu)}) ,\\ F(\mathbf{K})&=\sum_{k,k'}b_{k^{(\prime)}}e^{i\mathbf{K}\cdot\mathbf{r}_{k^{(\prime)}}^{(\nu)}} ,\end{aligned} \tag{4.11}$$

where $\mathbf{K}_h^{(\nu)}$ is the reciprocal-lattice point of the monoclinic lattice specified by $\beta_m^{(\nu)}$. Here, we have assumed that the domain sizes are of semimacroscopic scale, so that the spectra are simply expressed by the superposition of the intensities of individual Bragg reflections.

The result of the calculated spectrum along the $(40L)_m$ line is given in Fig. 8(a), in comparison with the observed spectrum. As is seen in the figure, there seem to be overall agreements. For instance, the observed directions of the tailing of the reflections $(404)_m$, $(403)_m$ and $(402)_m$ are consistently explained by the interpretation that the tail occurs towards the minor peak of the pair of reflections.

To be more quantitative, we estimate the peak shift $\Delta(L)$ defined by

$$\Delta(L)=\frac{\pm\Delta_0}{2}\left[\frac{|I_{(40L)}^{(1)}-I_{(40L)}^{(2)}|}{I_{(40L)}^{(1)}+I_{(40L)}^{(2)}}\right]^{1/2}\qquad(\pm:I^{(1)}\gtrless I^{(2)}) , \tag{4.12}$$

where $I^{(1)}(40L)$ and $I^{(2)}(40L)$ correspond to the intensities of the $(40L)_m$ reflection of the lattice (1) and the lattice (2), respectively, and Δ_0 is the splitting of the pair of Bragg reflections. The value $\Delta(L)$ is considered to define an "averaged" peak position by taking the weighted mean with respect to the intensities $I^{(1)}$ and $I^{(2)}$. The results are plotted in Fig. 8(b). The agreement is fairly good except for $(40\bar{1})_m$. We carried out a similar analysis for the $(20L)_m$ line. The agreements in the shift pattern $\Delta(L)$ are poorer, although qualitative features such as

tailing are consistent with the observed spectrum. We did not perform an analysis of the $(30L)_m$ and $(10L)_m$ lines because the Bragg intensities are sensitive to the additional parameter associated with the concentration distribution of Ni and Al on different sites.

V. SUMMARY AND DISCUSSIONS

We have developed a theoretical treatment of the martensitic phase transformation within a site-independent scheme to describe atomic fluctuations in a highly anharmonic lattice. From the microscopic standpoint, a pseudospin variable has been introduced which stands for the amplitude of a local vibrational mode called the "embryonic mode." The martensite structure is then characterized by the ferro-type ordered phase of the pseudospins. Through the coarse-graining procedure of the pseudospins, a semimacroscopic treatment has also been developed within the GL framework.

Both results were applied to the analysis of the martensite structure of the Ni-Al alloys. In particular, the anomalous features in neutron-diffraction spectra are understood by considering that the order parameter is spatially oscillating between two different values, which are interpreted in terms of the theoretically predicted crest-riding-periodon phase.

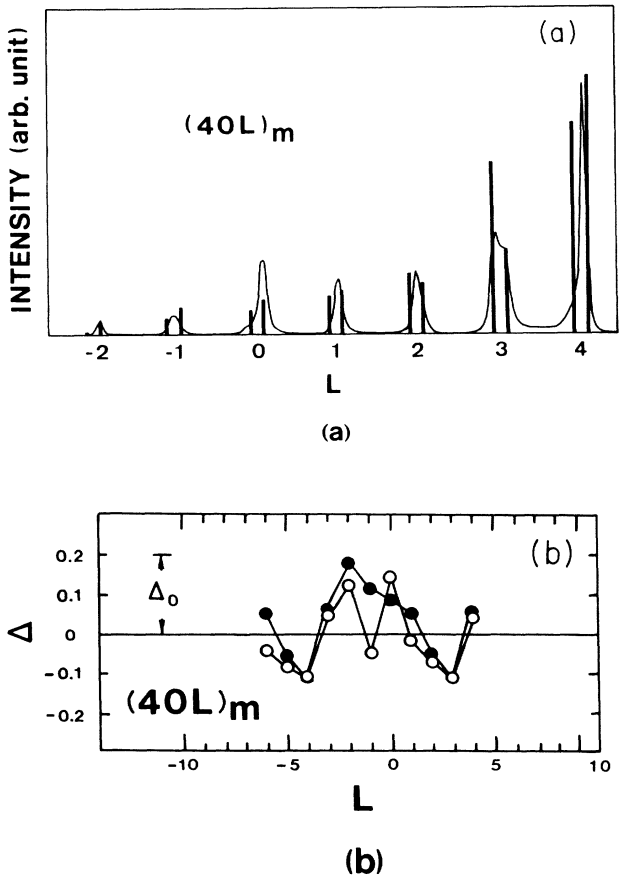

FIG. 8. (a) Comparison of the observed spectrum along the $(40L)_m$ line and the calculated $I(40L)_m$ of the CRP state by Eq. (4.11). (b) Comparison of the observed shift pattern along $(40L)_m$ line and the calculated $\Delta(40L)_m$ by Eq. (4.12).

As was pointed out in Sec. III, the observed order-parameter value is 0.48 relative to the perfect ($ABCABCB$) stacking of hexagonal basal planes. (See Table I.) Tadaki[24] also observed similar behavior in the so-called "9R" structure of the Cu-Zn alloy which exhibited a deviation from the ideal 9R structure. They discussed that the origin of this deviation is due to the difference of the atomic radius between Cu and Zn atom. From simple geometrical considerations, it was proved that, by taking the difference into consideration, the lattice will deviate from the exact orthorhombic system in accordance with the experimental results. Considering the appreciable difference in atomic radii between Ni and Al, the same arguments may also be at least partly applicable to the present case.

In the present treatment, we have ignored the atomic concentration fluctuations. Since the sample has the alloying ratio considerably off from nominal $Ni_{0.5}Al_{0.5}$ to construct the CsCl structure, the excess Ni atoms should be distributed more or less randomly on the Al site. It is quite possible that there is strong coupling between the concentration distribution of these excess Ni atoms and the structural characteristics. In fact, in the structure analysis of ζ-AgZn, Yamada and Noda[25] pointed out that the mass-density wave (MDW), which specifies the atomic concentration fluctuation, and the lattice distortion wave (LDW), which specifies the positional distortion, coexist side by side in Ag-Zn alloys.

When the r-dependent concentration $c(r)$ is taken into consideration in the present case, there would be an alternative interpretation of the coexistence of two slightly different monoclinic structures in NiAl as follows: After the heat treatment, the alloy tends to decompose into Ni-rich and Ni-deficient regions (spinodal decomposition). Through strong coupling between $c(r)$ and $\xi(r)$, such decomposition processes will eventually induce a "structural decomposition" which is equivalent to the CRP structure.

In this connection, the analysis of the spectra along the $[10L]_m$ and $[30L]_m$ lines would provide additional information concerning $c(r)$ because the structure factors of these reflections are sensitive to the atomic distribution on the sites within the basal plane. At the present stage, we cannot clearly distinguish from experimental evidences which is actually the major driving mechanism to stabilize the two-monoclinic mixed state.

APPENDIX

We consider a random system which is characterized by an irregular stacking of the equivalent basal planes defined by the unit-cell vectors (a_m, b_m). The structure factor of the system should be given by

$$F(\mathbf{K}) = F_l(\mathbf{K}) \sum_l e^{i\mathbf{K}\cdot\mathbf{r}_l} \delta(\hat{\mathbf{K}} - \hat{\mathbf{K}}_h) , \tag{A1}$$

where $F_l(\mathbf{K})$ is the "layer structure factor" of a single atomic plane and $\hat{\mathbf{K}}_h$ is a reciprocal-lattice point within

the (a_m^*, b_m^*) plane given by

$$\hat{\mathbf{K}}_h = H\mathbf{a}_m^* + K\mathbf{b}_m^*, \quad H \text{ and K are integers} . \tag{A2}$$

The coordinate r_i is the position vector drawn to the origin of the ith layer which will be generally expressed by

$$\mathbf{r}_i = x_i\mathbf{a}_m + z_i\mathbf{c}_m . \tag{A3}$$

Notice that, due to the random stacking, x_i and z_i are not integers but allowed to take arbitrary values.

The diffraction intensity is given by

$$I(\mathbf{K}) = |F_l(\hat{\mathbf{K}}_h)|^2 \sum_{i,i'} e^{i\mathbf{K}\cdot\mathbf{r}_{ii'}} , \tag{A4}$$

where the scattering vector is given by

$$\mathbf{K} = \hat{\mathbf{K}}_h + K_z\mathbf{c}_m^* . \tag{A5}$$

Notice again, K_z is not an integer.

As is pointed out in the text, the observed results show the following translational symmetry in the reciprocal space:

$$I(\mathbf{K} + 7\mathbf{c}_m^*) = I(\mathbf{K}) . \tag{A6}$$

Inserting $\mathbf{K} + 7\mathbf{c}_m^*$ for $\mathbf{K}$ in (A4), we have

$$I(\mathbf{K} + 7\mathbf{c}_m^*) = |F_l(\hat{\mathbf{K}}_h)|^2 \sum_{i,i'} e^{i\mathbf{K}\cdot\mathbf{r}_{ii'}} e^{2\pi i 7 z_{ii'}} . \tag{A7}$$

In order to satisfy the condition (A6), we should have

$$z_i = \tfrac{1}{7} \text{ (integer)} . \tag{A8}$$

Therefore, the translational symmetry (A6) is established when the layers are stacked with the same spacing of $\frac{1}{7}|c_m|\sin\beta_m$.

---

*Present address: Faculty of Science, Chiba University, Yayoi, Chiba 260, Japan.

†Present address: Department of Physics, Japan Atomic Research Institute, Tokai, Ibaraki 319-11, Japan.

[1]S. M. Shapiro, Materials Science Forum **56-58**, 33 (1990).

[2]M. Mori, Y. Yamada, and G. Shirane, Solid State Commun. **17**, 127 (1975).

[3]R. A. Robinson, G. L. Squires, and R. Pynn, J. Phys. F **14**, 1061 (1984).

[4]J. D. Axe, D. T. Keating, and S. C. Moss, Phys. Rev. Lett. **35**, 530 (1975).

[5]W. Petry, T. Flottmam, A. Heiming, J. Trampenau, M. Alba, and G. Vogl, Phys. Rev. Lett. **61**, 722 (1988).

[6]S. M. Shapiro, J. Z. Larese, Y. Noda, S. C. Moss, and L. E. Tanner, Phys. Rev. Lett. **57**, 3199 (1986).

[7]V. Y. Martynov, K. Enami, L. G. Khandros, S. Nenno, and A. V. Tkachenko, Phys. Met. Metallogr. (USSR) **55**, 136 (1983).

[8]G. S. Zhdanov, Dokl. Akad. Nauk USSR **48**, 39 (1945).

[9]Y. Noda, S. M. Shapiro, G. Shirane, Y. Yamada, K. Fuchizaki, and L. E. Tanner, Materials Science Forum **56-58**, 299 (1990).

[10]Y. Noda, S. M. Shapiro, G. Shirane, Y. Yamada, and L. E. Tanner, preceding paper, Phys. Rev. B **42**, 10 397 (1990).

[11]K. Fuchizaki, Y. Noda, and Y. Yamada, Phys. Rev. B **39**, 9260 (1989).

[12]Y. Yamada, K. Fuchizaki, and Y. Noda, Materials Science Forum **56-58**, 107 (1990).

[13]A. D. Bruce, Adv. Phys. **29**, 111 (1980).

[14]R. M. Wentzcovitch and M. L. Cohen, Phys. Rev. B **37**, 5571 (1988).

[15]K. Fuchizaki, Ph.D. thesis, Osaka University, 1989 (unpublished).

[16]P. Bak and J. von Boehm, Phys. Rev. B **21**, 5297 (1980).

[17]J. W. Cahn and J. E. Hilliard, J. Chem. Phys. **31**, 688 (1959).

[18]F. Falk, Z. Phys. B **51**, 177 (1983).

[19]A. E. Jacobs, Phys. Rev. B **31**, 5984 (1985).

[20]G. R. Barsch, J. A. Krumhansl, L. E. Tanner, and M. Wuttig, Scr. Metall. **21**, 1257 (1987).

[21]G. R. Barsch and J. A. Krumhansl, Metall. Trans. **19A**, 761 (1988).

[22]In this representation, one of the off-diagonal tensor component is asymmetric ($\epsilon_{13} \neq \epsilon_{31}$). This is simply due to the fact that we took the $\mathbf{e}_1$ direction unchanged during the deformation.

[23]Recently, another example of the CRP phase has been observed in the fcc-based FePd alloy: H. Seto, Y. Noda, and Y. Yamada, J. Phys Soc. Jpn. **57**, 3668 (1988).

[24]T. Tadaki, M. Tokoro, and K. Shimizu, Scr. Metall. **8**, 1077 (1974).

[25]Y. Yamada and Y. Noda, J. Phys. Soc. Jpn. **57**, 1303 (1988).

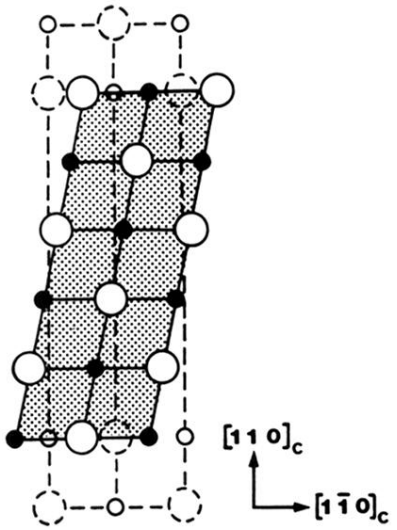

FIG. 1. The embryonic mode postulated from the soft phonon in NiAl. The mode is characterized by the "tilting" motion of a cluster composed of six $(110)_c$ layers.

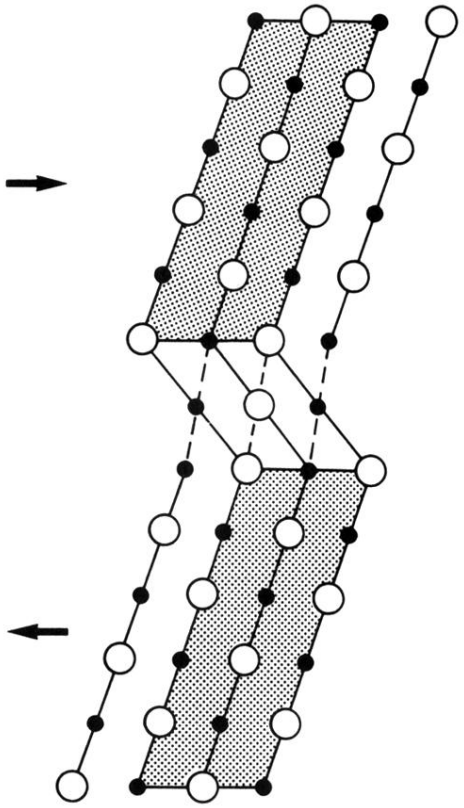

FIG. 3. Origin of the coupling between Q^{emb} and Q^{tr}. The translation of the neighboring clusters in the opposite directions as shown by the arrows is favorable for the same tilted configuration ($\sigma = 1$) of the clusters (and vice versa) because the atomic positions at the interface layers come too close to each other without this translation.